

HYDRAULICS OF RUBBER DAM OVERFLOW : A SIMPLE DESIGN APPROACH

H. CHANSON

Department of Civil Engineering, The University of Queensland, Brisbane QLD 4072, AUSTRALIA

ABSTRACT

Rubber dams have been used for the past 40 years in river and coastal engineering applications, in Australia and overseas. Despite the increasing interest for rubber dams, little information is available on their hydraulic performances. The overflow characteristics of inflated rubber dams are re-investigated. New analytical calculations provide information on the wall pressure distribution and on the nappe trajectory. The calculations are compared with over 160 new experiments. Altogether the results provide a new method to predict overflow characteristics and new design guidelines are derived for the optimum location of the deflector.

INTRODUCTION

Rubber dams are long tubular-shaped fabrics placed across channels, streams and weir crest to raise the upstream water level when inflated (Fig. 1). In open channels, they are commonly used to raise water levels, to increase water storage and to prevent chemical dispersion (Table 1). The interest in inflatable dams is increasing because of the ease of placement. Such structures can be installed during later development stages.

The membrane is usually deflated for large overflows. It is however common practice to allow small spillages over the inflated dam. During overflows, vibrations might result from fluid-structure interactions (e.g. OGIHARA and MARAMATSU 1985, WU and PLAUT 1996), and the instabilities might damage and destroy the rubber membrane. Several failures were experienced including in Australia. In practice, a deflector (i.e. fin) is installed on the downstream face of the rubber dam to project the nappe away from the membrane, hence preventing rubber membrane vibrations (Fig. 2).

Little attention has been paid on the overflow hydraulics. ANWAR (1967) investigated experimentally small overflow. Other studies (e.g. SHEPHERD et al. 1969, BINNIE et al. 1973) discussed the fluid-structure interactions of inflated rubber dams.

In the present paper, the characteristics of rubber dam overflow are re-investigated. New analytical calculations of nappe trajectory are presented and the results are compared with laboratory experiments. New guidelines for the optimum design of rubber dam deflector are discussed.

NAPPE TRAJECTORY

Considering a fully-inflated rubber dam, the downstream face of the dam follows closely the shape of a circular cylinder as observed by ANWAR (1967). For the sake of simplicity, we shall consider an idealised rubber dam shape (Fig. 2).

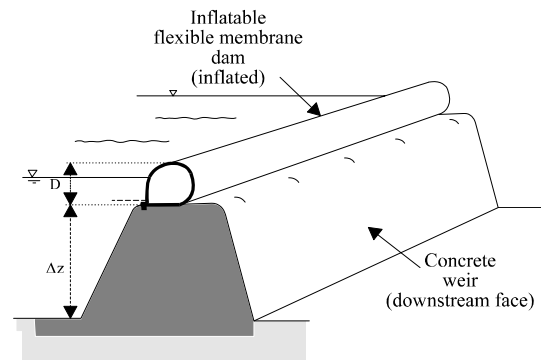


Fig. 1: Sketch of a rubber dam

Year	Site	Characteristic s	Manufactur er	Remarks
(1)	(2)	(3)	(4)	(5)
1965	Koomboolo omba dam, QLD	$L = 1 \times 60$ m, $D = 1.22$ & 1.5 m, $H_{infl} =$ 0.91 m	Fabridam- Firestone	No deflector. Water filled. Placed on ogee crest. Design overflow : 2.4 m ² /s (inflated), 35 m ² /s (deflated).
1967	Proston weir, QLD	$L = 1 \times 51$ m, $D = 1.5$ m, $H_{infl} = 1.4$ m	Fabridam- Firestone	No deflector. water filled
1983	Val Bird weir, North QLD	$L = 2 \times 82$ m, $D = 1.9$ m, $H_{infl} = 0.5$ m	Fabridam- Firestone	Water filled.
1996	Lyell dam, NSW	$L = 2 \times 40$ m, $D = 3.5$ m, $H_{infl} = 1.4$ m	Bridgestone	With deflector. Air filled
1997	Dumbleton weir, Central QLD	$L = 2 \times 75$ m, $D = 2$ m $H_{infl} = 0.7$ m	Queensland Rubber Co.	With deflector. Air filled.

Table 1: Examples of rubber dams installed in Australia

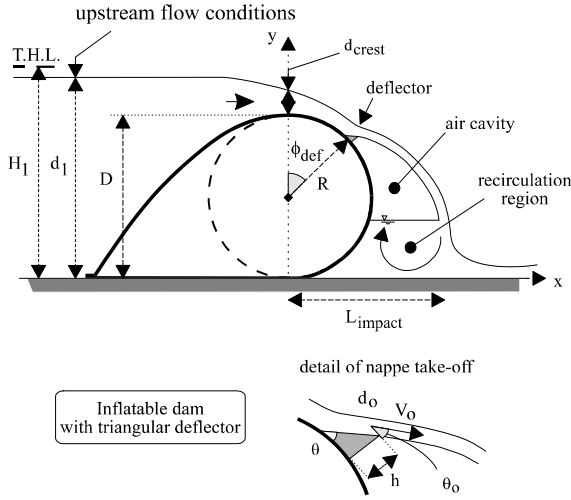


Fig. 2: Rubber dam overflow

Downstream of the crest, the overflowing nappe adheres to the weir face because the convex wall curvature imposes a pressure field modification within the nappe inducing a suction pressure. The resulting Coanda effect acts on the wall surface in a direction normal to the flow direction.

At the crest, critical flow conditions occur. Downstream of the crest, the flow depth and velocity derive from the continuity and motion equations. Assuming an ideal-fluid flow, it yields :

$$F = \sqrt{F_{crest}^2 + 2 * (1 - \cos\phi)} \quad (1)$$

$$\frac{d}{R} = \left(\frac{d_{crest}}{R}\right)^{3/2} * \frac{C_D}{k^{3/2}} * \frac{1}{F} \quad (2)$$

where d is the flow depth, V is the velocity, $F = V/\sqrt{g^*R}$, ϕ is the angular position, $F_{crest} = V_{crest}/\sqrt{g^*R}$, C_D is the discharge coefficient, H_1 is the upstream total head, D is the dam height, d_{crest} is the flow depth at the crest, R is the radius of curvature and $k = d_{crest}/d_c$ accounts for the streamline curvature and non-uniform distributions of pressure and velocity at the crest (Fig. 2).

At the surface of the rubber dam, the wall pressure may be deduced from the motion equation in the radial direction. At any position ϕ , the dimensionless pressure distribution at the wall equals :

$$\frac{P_{atm} - P_s}{\rho_w * g^* R} = \frac{d}{R} * \left(F^2 - \cos\phi * \left(1 + \frac{d}{2 * R}\right)\right) \quad (3)$$

where P_s is the absolute pressure at the wall, P_{atm} is the atmospheric pressure, ρ_w is the water density. Equation (3) predicts an increasing suction pressure ($P_{atm} - P_s$) down the rubber membrane as the flow is accelerated.

The nappe adherence on the wall might lead to flow instability at the base of the nappe (i.e. next to the separation position), pressure fluctuations on the downstream face of the dam and vibrations of the flexible membrane. Nappe adherence instabilities may be eliminated by deflecting the nappe off the rubber wall (Fig. 2).

At take-off the flow properties (d_o , V_o , θ_o) are deduced from the Bernoulli and continuity equations, neglecting energy losses and assuming that the effects of the developing boundary layer are small (i.e. Eq. (1) and (2)). Usually the

deflected nappe angle θ_o at take-off is smaller than the deflector angle θ , and it may be estimated in first approximation as :

$$\frac{\theta_o}{\theta} = \sqrt{\tanh\left(\frac{h}{d_o * \theta}\right)} \quad (4)$$

where h is the deflector height measured normal to the wall and d_o is the nappe thickness at take-off (Fig. 2).

The trajectory equations of a ventilated nappe are :

$$\frac{x}{R} = \frac{V_o}{\sqrt{g^*R}} * \cos(\phi_{def} - \theta_o) * \sqrt{\frac{g^* t^2}{R}} + \frac{x_o}{R} \quad (5)$$

$$\frac{y}{R} = -\frac{1}{2} * \frac{g^* t^2}{R} - \frac{V_o}{\sqrt{g^*R}} * \sin(\phi_{def} - \theta_o) * \sqrt{\frac{g^* t^2}{R}} + \frac{y_o}{R} \quad (6)$$

where x is the horizontal direction, y is the vertical direction positive upwards, t is the time, x_o and y_o are the co-ordinates of the deflector edge, ϕ_{def} is the angular position of the deflector.

Equations (1) to (6) may be combined to predict the nappe trajectory from the crest down to the nappe impact.

COMPARISON WITH EXPERIMENTAL DATA

Experimental setup

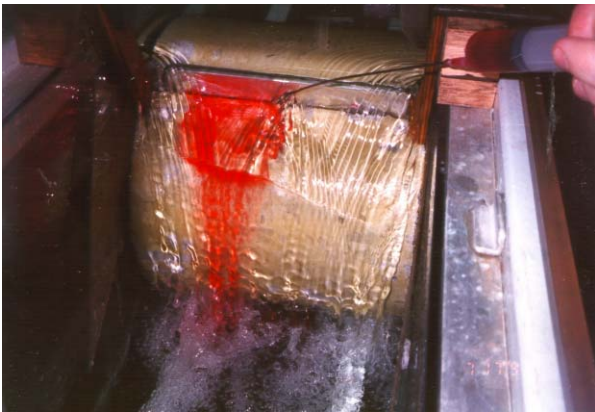
Laboratory experiments were conducted to validate qualitatively and quantitatively the basic flow patterns. The inflated rubber dams were idealised with circular concrete cylinders (Fig. 3). Two rectangular channels were used. Each flume is supplied with recirculating water supplied by a constant head tank, the discharge being measured by 90-degree V-notch weirs.

Several configurations were tested : i.e., three cylinder sizes ($R = 0.052, 0.0755, 0.117$ m), several deflector sizes and positions ($0 \leq h \leq 0.11$ m, $0 \leq \phi_{def} \leq 90$ deg.). All cylindrical weirs had a smooth varnish surface and the deflected napped were ventilated by sidewall splitters. The flow depths were measured on the centreline using point gauges connected to a Mitutoyo™ digimatic caliper (Ref. No. 500-171). The error on the flow depth was less than 0.1-mm and the error on the longitudinal position was less than 0.5 mm.

The hydraulic characteristics of the crest were investigated separately and results were presented in CHANSON and MONTES (1997). The present experimental study was focused on the nappe trajectories and altogether over 160 new experiments were performed.



(A) Flow from right to left : $q = 0.0048 \text{ m}^2/\text{s}$, $d_1 = 0.178 \text{ m}$, $R = 0.117 \text{ m}$, $\phi_{\text{def}} = 45 \text{ deg.}$, $h = 0.004 \text{ m}$



(B) Nappe re-attachment : $q = 0.006 \text{ m}^2/\text{s}$, $W = 0.25 \text{ m}$, $R = 0.117 \text{ m}$, $\phi_{\text{def}} = 25 \text{ degrees}$, $h = 0.026 \text{ m}$

Fig. 3: Overflow above an ideal rubber dam with deflector

Experimental results

Visual observations (e.g. Fig. 3) showed satisfactory operation of the rectangular deflectors. Upstream of the fin, the nappe accelerates until it is projected upwards. Once deflected, the flow becomes a free-falling nappe. The jet trajectory depends critically upon the location ϕ_{def} of the deflector. Further the trajectory expands with increasing deflector height h for the same weir, flow conditions and deflector location ϕ_{def} .

Note that the deflector induced a backwater effect upstream for $\phi_{\text{def}} = 0$ ($h/R > 0$, all flow rates) and $\phi_{\text{def}} = 25 \text{ degrees}$ ($h/R \geq 0.22$, all flow rates) only. For these geometries, critical flow conditions occurred at the deflector rather than at the crest.

Careful measurements of the upper nappe and recirculation pool were performed and compared with ideal-fluid flow calculations (e.g. Fig. 4).

Overall reasonable agreement was found between calculations and data, but for the smaller cylinder size (i.e. $R = 0.0524 \text{ m}$). For $R = 0.0524 \text{ m}$, the deflected nappe tended to attach to the fin, leading to shorter jet trajectories than predicted in some tests.

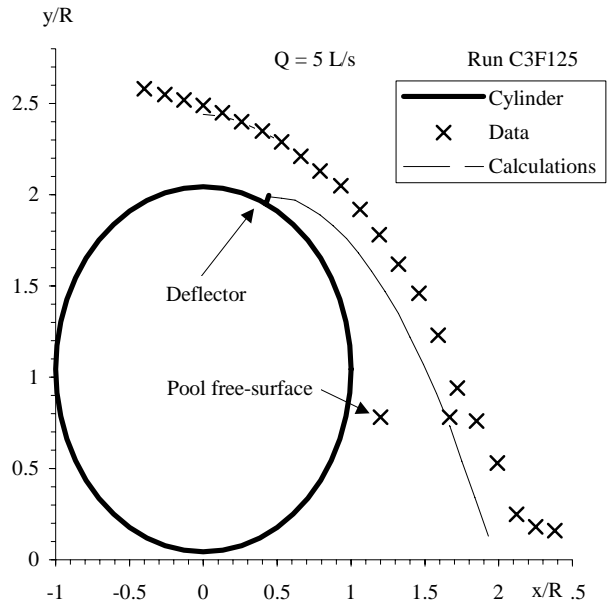


Fig. 4: Nappe trajectories - Comparison between experimental data and ideal-fluid flow calculations
 $\phi_{\text{def}} = 25 \text{ deg.}$, $q = 0.020 \text{ m}^2/\text{s}$, $R = 0.0755$, $d_1 = 0.2012 \text{ m}$, $h = 0.0039 \text{ m}$, $D = 0.1544 \text{ m}$, $d_{\text{crest}} = 0.03305 \text{ m}$

Comparison with air jet studies

Several researchers investigated the Coanda effect with air jets flowing past circular cylinders. FEKETE (1963) performed very careful pressure measurements with various cylinder diameters ($1.2\text{E}+5 < \rho \cdot V \cdot R / \mu < 7.4\text{E}+5$) while SARPKEYA (1968) investigated the deflection of air jets blowing past circular quadrants ($2.45\text{E}+5 < \rho \cdot V \cdot R / \mu < 4.0\text{E}+5$). A re-analysis of their data (Fig. 5) indicates that the dimensionless pressure distributions on the cylinder wall were close to ideal-fluid flow calculations :

$$\frac{P_{\text{atm}} - P_s}{\rho \cdot g \cdot R} = F^2 \cdot \frac{d}{R} \quad \text{Air flow (3b)}$$

where V , F and d are defined in terms of the flow properties at the jet nozzle, and ρ and μ are the fluid density and viscosity respectively. Equation (3b) is compared favourably with the original data of FEKETE (1963) and SARPKEYA (1968) on Figure 5.

Nappe re-attachment

The agreement between data (air jets and water nappes) and calculations suggests that the ideal-fluid flow calculations may be used as a design tool to predict the optimum deflector position and size and to calculate the corresponding nappe trajectory.

The purpose of the fin being to deflect the nappe away from the wall, nappe re-attachment downstream of the deflector is not acceptable. In laboratory, nappe re-attachment was observed for $\phi_{\text{def}} = 0$ (all flow rates) and for $\phi_{\text{def}} = 25 \text{ degrees}$ at low flow rates (e.g. Fig. 3B). No nappe re-attachment was observed for $\phi_{\text{def}} = 30$ to 90 degrees . However, with $\phi_{\text{def}} = 90 \text{ degrees}$, little nappe deflection was observed and the nappe impact was located not far away from the rubber dam toe.

Overall maximum nappe deflection was observed for $30 \leq \phi_{\text{def}} \leq 60$ degrees. This result is very close to calculations (CHANSON 1996).

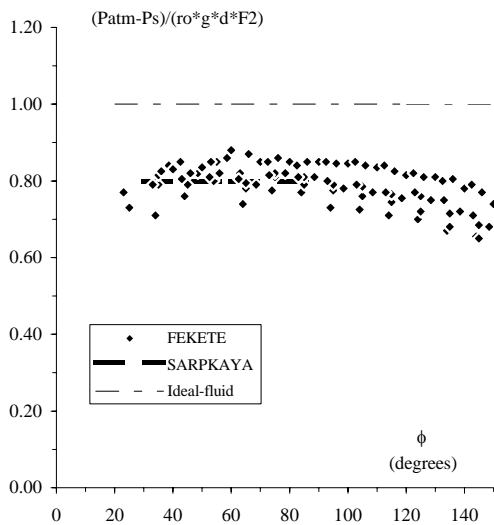


Fig. 5: Adherence pressure distribution $(P_{\text{atm}} - P_s) / (\rho * g * d * F^2)$ versus ϕ - Comparison with air jet data

SUMMARY AND CONCLUSION

Overflow of rubber dams is characterised by an accelerating nappe which adheres to the membrane wall. Hydrodynamic and fluid-structure instabilities may develop and must be avoided. Current design techniques include the installation of a fin on the upper quadrant of the rubber dam, to deflect the flow away from the flexible membrane wall.

Analytical calculations have been developed to predict the nappe trajectory above rubber dams, including the free-falling jet. The results have been compared successfully with experimental data. The ideal-fluid flow calculations may be used by designers to predict the nappe trajectories and to prevent nappe re-attachment situations. The new laboratory experiments and calculations (CHANSON 1996) have been used also to show that the optimum location of the deflector is $30 \leq \phi_{\text{def}} \leq 60$ degrees.

A major limitation of the present work is the assumption of steady flow and boundary conditions. Rubber dams are made of flexible membranes which respond to hydrodynamic fluctuations (e.g. wall turbulence). The shape of the rubber dam is also a function of the upstream head and this was ignored.

ACKNOWLEDGMENTS

The author acknowledges the assistance of his former students R. McCONAGHY, A. SWINCER, E. SHAW and T. SIAW.

REFERENCES

- ANWAR, H.O. (1967). "Inflatable dams." *Jl of Hyd. Div.*, ASCE, Vol. 93, No. HY3, pp. 99-119.
- BINNIE, G.M., THOMAS, A.R., and GWYTHYER, J.R. (1973). "Inflatable Weir used during Construction of Mangla

Dam." *Proc. Instn. Civ. Eng.*, Part 1, Vol. 54, Nov., pp. 625-639. Discussion : 1974, Part 1, Vol. 56, pp. 189-194.

CHANSON, H. (1996). "Some Hydraulic Aspects during Overflow above Inflatable Flexible Membrane Dam." *Report CH47/96*, Dept. of Civil Engineering, University of Queensland, Australia, May, 60 pages.

CHANSON, H., and MONTES, J.S. (1997). "Overflow Characteristics of Cylindrical Weirs." *Research Report No. CE154*, Dept. of Civil Engineering, University of Queensland, Australia, 96 pages.

FEKETE, G.I. (1963). "Coanda Flow of a Two-Dimensional Wall Jet on the Outside of a Circular Cylinder." *Report No. 63-11*, Dept. of Mech. Eng., McGill University, Canada.

OGIHARA, K., and MARAMATSU, T. (1985). "Rubber dam : Causes of Oscillation of Rubber Dams and Countermeasures." *Proc. 21st IAHR Congress*, Melbourne, Australia, pp. 600-604.

SARPKEYA, T. (1968). "The Deflection of Plane Turbulent Jets by Convex Walls." *US Govt Research Report No. AD 673249*, Naval Postgraduate School, Monterey CA, USA.

SHEPHERD, E.M., McKAY, F.A., and HODGENS, V.T. (1969). "The Fabridam Extension on Koombooloomba Dam of the Tully Falls Hydro-Electric Power Project." *Jl Instn. of Eng., Australia*, Vol. 41, pp. 1-7.

WU, P.H., and PLAUT, R.H. (1996). "Analysis of the Vibrations of Inflatable Dams Under Overflow Conditions." *Thin-Walled Structures*, Vol. 26, No. 4, pp. 241-259.